

DOI: <http://doi.org/10.32792/utq.jceps.12.01.02>

## Synthesis and Characterization of Nanosized Iron Using Three Different Methods

Dr. Wed Al-Graiti\*<sup>1</sup>, Prof. Dr. Mohsin Al-Dokheily<sup>2</sup>, Prof. Dr. Mahmood Shakir Magtoof<sup>2</sup>

<sup>1</sup>College of Dentistry, University of Thi-Qar, Thi-Qar, 64001, Iraq

<sup>2</sup>Department of Chemistry, College of Science, University of Thi-Qar, Thi-Qar, 64001, Iraq

Received 11/5/2021 Accepted 11/11/2022 Published 30/3/2022



This work is licensed under a [Creative Commons Attribution 4.0 International License](https://creativecommons.org/licenses/by/4.0/).

### Abstract:

Concerns about water pollution keep growing locally and around the world in regards the advanced industries and related all life aspects health. Every day, the industries activity ends in depositing contaminants into a water source or connected aqua systems. The contamination is getting widely distributed, so the demand for cost-effective, efficient, and advanced system for water pollution remediation is needed as traditional remediation processes were relatively weak. Nano zero valent iron synthesized by sodium borohydride has an outstanding reactivity and abundancy. It has a great surface area to volume ratio with strong reactivity. Recently, the potential reducing property of nano-scale zero valent iron, NZVI, has attracted much more attention and many studies used NZVI for the reduction of organic and inorganic contaminants in aquatic environment. It can also be used for the remediation of groundwater and removal of heavy metals from industrial wastes. Therefore, it is synthesized in current paper and characterized by BET, XRD, and IR spectroscopic technologies.

**Keywords:** Nanotechnology, sodium borohydride, Adsorption, Zero valent iron

### 1. Introduction:

Nanotechnology is a low cost and useful engineering technology demonstrated by the particles at the nanoscale ( $1\text{nm}=10^{-9}\text{m}$ ) [1, 3] Nanotechnology brought new application and challenges for iron at environmental remediation [2, 4, 5]. It has a great surface area to volume ratio with strong reactivity. This is because the surface area can be increased by decreasing the diameter of the particle from micro (for example) to nano. Moreover, larger surface area leads to greater reactivity as the reactive site at the surface increases significantly [6]. Recently, the potential reducing property of nano-scale zero valent iron, NZVI, has attracted much more attention [7, 8] and many studies used NZVI for the reduction of organic and inorganic contaminants in aquatic environment [3, 9, 10]. It can also be used for the remediation of groundwater and removal of heavy metals from industrial wastes [11].

several methods were published for the synthesis of NZVI with possible modification of surface properties for better reducing performance. This study delivers three procedures of NZVI synthesis using sodium borohydride. Synthesis conditions assessed to select the best yield and powder properties of NZVI.

### 2. Materials and Methods:

**2.1. Materials:** Ferrous sulphate hydrate  $\text{Fe}_2\text{O}_3 \cdot 18\text{H}_2\text{O}$ , and sodium borohydride  $\text{NaBH}_4$  were purchased from Fluka company. Ferric chloride  $\text{FeCl}_3$  was obtained from BDH company. In addition, methanol  $\text{CH}_3\text{OH}$ , ethanol  $\text{C}_2\text{H}_5\text{OH}$ , and silica gel (mesh = 60-120) were provided from Merck company.

For physical characterization, a number of equipments was used including XRD-6000 Shimadzu (made in Japan), HPLC D-star instruments (made in England), and NOVA 2200 BET-surface area analyzer (made in Rome). Also, ultra sonic model nu:FS100b (made in England). In addition, metallurgical microscope model beam rmm-7t (2003) (made in India).

## 2.2. Synthesis Methods of Nano Zero Valent Iron Powder:

**First Method (figure 1):** to start the synthesis procedure, 10g of ferrous sulphate hydrate  $\text{Fe}_2\text{O}_3 \cdot 18\text{H}_2\text{O}$  was dissolved in a %30 methanol/DI water mixture and stirred well. 5M of sodium hydroxide  $\text{NaOH}$  was prepared and 10 ml was taken and poured into the previous mixture to reach PH 6.1. 50ml of sodium borohydride  $\text{NaBH}_4$  2.1M was added (0.5ml per second by a burette) (for better yield of ZVI excessive amount of  $\text{NaBH}_4$  is needed). The mixture was left for 5 minutes to release the bubbles as reduction reaction takes place immediately after dropping the first drop of the borohydride where the black particles of NSZVI start appearing. Later, the mixture was transferred into the test tubes which were placed inside the centrifuge at 6000 cycle per minute for 5 minutes approximately. At the end of centrifuging, two phases would be obtained, separate the nanoparticles from the liquid phase (decantation) then transfer the black particles to a watch glass which would be finally dried in the oven overnight at  $105^\circ\text{C}$ . This sample will be referred as sample (1) within the text.

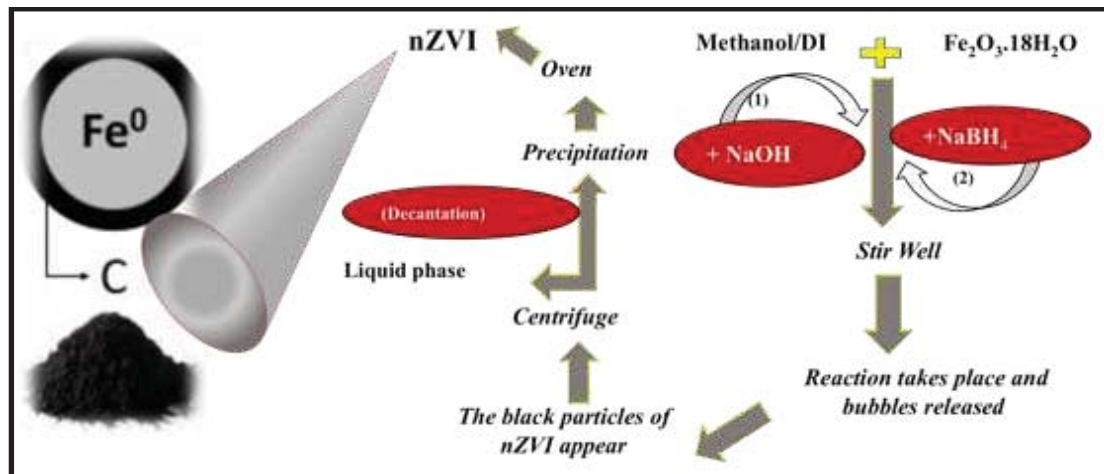


Figure (1) Schematic illustration of preparation method of NZVI

**Second Method:** 10g of ferrous sulphate hydrate ( $\text{Fe}_2\text{O}_3 \cdot 18\text{H}_2\text{O}$ ) was dissolved in a %30 methanol/DI water mixture and mixed well. 4g of silica gel was weighed and added to the previous mixture. The PH meter was already inserted in the prepared mixture to adjust the PH reading at 6.8 after adding the base 3.8M. Then, 1.8g of  $\text{NaBH}_4$  was gradually added to the components of the mixture, when completed, the bubbles released from the reaction happening upon mixing the previous materials. The mixture was stirred for 20 minutes and transferred into test tubes to be placed inside centrifuge at 4000 cycle per minute ended up with two phases (liquid phase and a black precipitation). The black particles were separated from the liquid phase (decantation) and dried at desecator. This sample will be referred as sample (2) within the text.

**Third Method:** 0.2M of sodium borohydride  $\text{NaBH}_4$  was prepared and poured to 0.05M of ferric chloride 1:1 ratio. The mechanism of the reaction can be written as following:



This sample will be referred as sample (3) within the text.

### 2.3. Physical Characterization of Nano-sized Zero Valent Iron Particles:

X-ray diffraction measurements were done using XRD-6000 shimadzu equipment. BET test, measuring the surface area, was also done by placing NZVI powder in a long tube where  $\text{N}_2$  gas inserted inside the tube to absorb onto the active sites at the particles surface. By increasing the temperature, a specific volume of  $\text{N}_2$  gas released and measured to be the initial absorbed layer  $V_{\text{mon}}$ . Increasing the pressure continuously (feeding more  $\text{N}_2$  gas), increases the absorbed layers of  $\text{N}_2$ . Consequently, the measured volume this time can be reflected as a second absorbed layer of  $\text{N}_2$  gas onto NZVI active sites. It has been approved that, NZVI particles have the potential to undergo multiple absorbed layers. Also, optical microscope has been employed in current study (**figure 3**). After setting up the microscope, NZVI powder prepared via first method were placed on a glass slide (scaled) to be examined under 10X zoomed screen. The photos of the examined sample were taken and saved using a digital camera. The same procedure was repeated for the NZVI powder prepared by the second method and 49X was set as zoomed power of the digital camera.

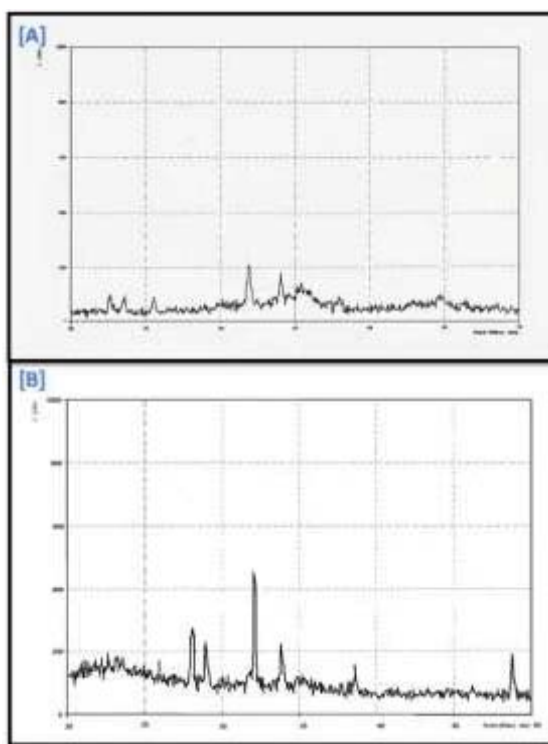


Figure (2) XRD charts of NZVI samples prepared via: [A] First synthesis method (sample 1). [B] Second synthesis method (sample 2).

Figure 3 A&B illustrates the digital photos were taken to NZVI, samples 1&2, to investigate the surface and powder features. Both samples were distributed in a very small quantity (aggregated

molecules) which made it hard to check the molecules without the need to zoom in. First sample, figure 2A, was zoomed up to 10X times, then, the separated quantities of NZVI were seen by a digital camera, even though, the vision was a bit blurry. Each line equaled to 166nm and the NZVI molecules were even smaller than that scale which confirms the nano size of tested NZVI molecules belong to sample1. Figure 2B, indicates the size of NZVI molecules of sample 2. The second sample was examined under 49X zoomed power. It verifies the nano size of NZVI molecules as each line equals to 700 nm, and undoubtedly, the molecules were much smaller than the set scale.

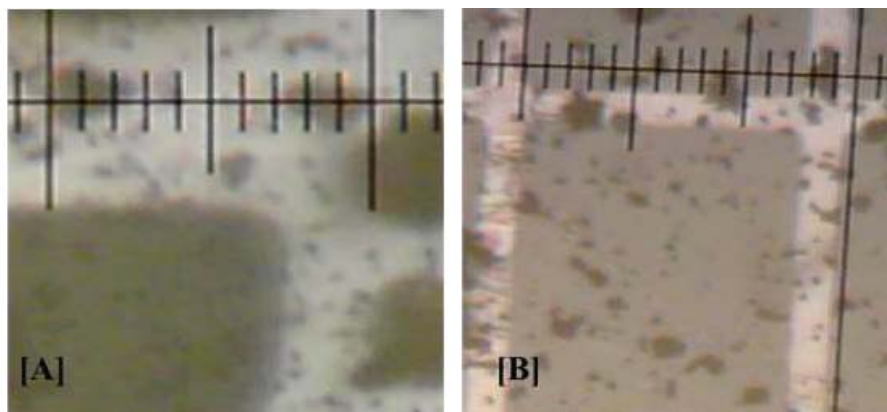


Figure (3) Digital photos of NZVI powder. [A] Each line equals to 166 nm (sample 1). [B] Each line equals to 700 nm (sample 2).

### 3. Results and Discussion:

#### 3.1. Samples of NZVI Powder Prepared in Current Study:

According to conducted synthesis methods of NZVI in our lab (methods listed in section 2.2), it can be said that, first synthesis method has given a black powder with (% 14.7) yield (sample 1). Also, a brown powder with (% 25.9) yield of NZVI was produced by the second synthesis method (sample 2). While the third synthesis method gave a black powder fastly oxidized (turned to rust) with % 6.9 yield (sample 3) which is not enough for aimed applications or characterization.

As mentioned earlier, NZVI synthesis was done by several methods. Some of them apply reduction reaction using sodium borohydride or hydrogen reduction where ferros ( $\text{Fe}^{+2}$ ) is heated up with sodium borohydride at 400 C° to give ferros oxide. When ferros oxide is formed, it would then be reduced by hydrogen at 500 C° to finally produce NZVI particles with high porosity.

#### 3.2. X-Ray Diffraction:

A couple of XRD results were comprehensively interpreted here. **Figure 2 (A & B)** is obtained from NZVI samples synthesized via first and second methods (samples 1 & 2 as explained in 2.2 section). The results showed that, NZVI sample prepared via first method (sample 1) using ferrous sulphate (0.3 M) had a peak at  $2\Theta = 44.63$  (figure 3A). The thickness of this peak was %27 which suggests the presence of  $\alpha$  Fe known as ferrite. Two main peaks were noticed at  $2\Theta = 31.95$  and  $2\Theta = 34.07$  in addition to other peaks with less thickness appeared at  $2\Theta = 23.95, 25.58, 34.6, 35.1, 35.3,$  and  $35.7$ . All these peaks confirm the main phase of tested sample of NZVI which is  $\epsilon\text{-Fe}_2\text{O}_3$  (epsilon iron oxide) as referred by Forestier and Guillain in 1934. In 1998, Tronc and his colleagues had the opportunity to distinguish the

structure of  $\epsilon$ -Fe<sub>2</sub>O<sub>3</sub>, also, Klem and Mader approved same structure of  $\epsilon$ -Fe<sub>2</sub>O<sub>3</sub> in 2005. Furthermore, in 2002 Zboril and his friends referred to the formation of  $\epsilon$ -Fe<sub>2</sub>O<sub>3</sub> when  $\gamma$ -Fe<sub>2</sub>O<sub>3</sub> transfers to  $\alpha$ -Fe<sub>2</sub>O<sub>3</sub>.

It's worth mentioning that, iron oxide type ( $\epsilon$ ) possesses a crystal structure "orthorhombic" at room temperature. This shape can be defined by unequal sides, however, it showed equal angles 90°. Regards this geometry, the oxide forms closed layers set on top of each other in sequential order, while Fe ions occupy the spaces at the corners of tetrahedral or octahedral crystal system.

In the same hand, **figure 2B** shows the XRD result of NZVI prepared by the second method (sample 2). The three prominent peaks at  $2\Theta = 32.14, 28.07$  and  $29.004$ , in addition to, less thickness peaks appeared at  $2\Theta = 31.89, 33.68, 33.87,$  and  $38.64$  confirm the existence of iron oxide type ( $\epsilon$ ).

### 3.3 BET Results:

Fe<sup>0</sup> particles prepared by first method had a surface area = 22.6 g/m<sup>2</sup> which is approaching to was already mentioned by Liu and his friends [9]. Fe<sup>0</sup> particles prepared by second method were also examined by BET test for the same purpose. About 278.232 g/m<sup>2</sup> was the surface area of Fe<sup>0</sup> particles and this is much higher than surface area of Fe<sup>0</sup> particles prepared by Ponder and his co-workers. The difference between surface area prepared by the first and second methods could be attributed to using silica gel as supporting material during preparation process and that can increase the surface area in return. Ponder from his side used "resin" as supporting material when he synthesized Fe<sup>0</sup> particles, so a minor increase of the surface area has been noticed. The relationship between applied pressure and released volumes for the prepared samples can be shown as following:

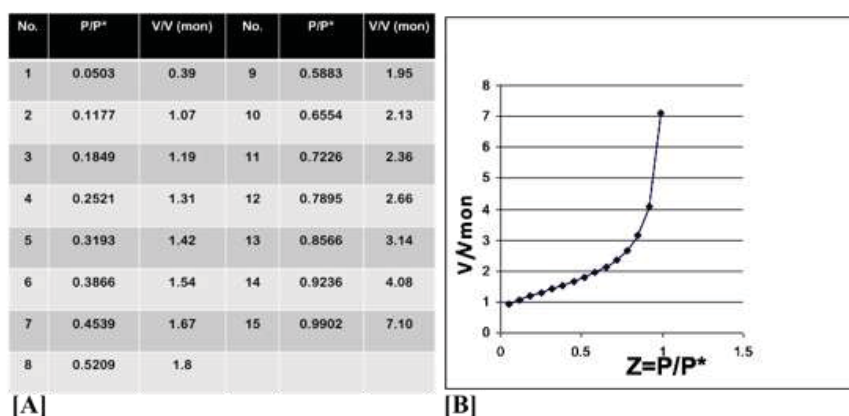


**Figure (4) [A] “Isothermal adsorption of Fe<sup>0</sup> prepared via first method, [P/P\* = relative pressure] and [V/V<sub>mon</sub> = volume adsorbed]”. [B] “relationship between pressure and adsorbed layer on top of iron’s surface sample (1)”**

Prepared particles of Fe<sup>0</sup> were having approximately the same readings of adsorbed layers as shown in **figure 4** (1-13 readings), Therefore, first 13 readings together can form the first adsorbed layer on particles surface. At reading 14, the adsorption curve was clearly elevated and that confirms the creation of more adsorbed layers on surface of Fe<sup>0</sup> particles. Moreover, continuously increasing the gas pressure made a noticeable change to adsorption process by increasing the volume of released gas. This behavior can be seen between 14 and 15 readings in figure 4 where the adsorption curve has a strong lifting. Notably, the Fe<sup>0</sup> particle size was equal to 6.29 nm. When the adsorption curve was then set using the data obtained by PONDER synthesis method, the adsorption results were different to what we had before as explained in **figure 5**.

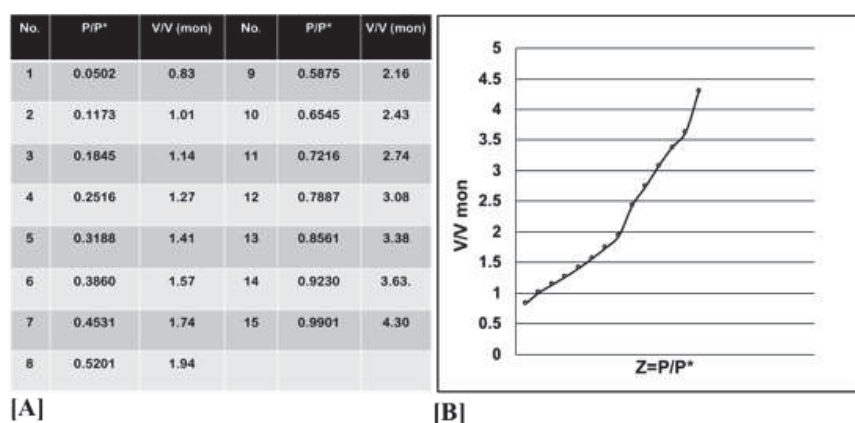


Figure (5) [A] “Isothermal adsorption of Fe<sup>0</sup> prepared via second method, [P/P\* = relative pressure] and [V/V<sub>mon</sub> = volume adsorbed]”. [B] “relationship between pressure and adsorbed layer on top of iron’s surface sample (2)”

In this curve, all the readings are in a state of raising. As can be seen, after each reading, the adsorption curve kept lifting all along. This shows the multiplicity of adsorbent layers which were build up at particles surface. it can be said that, based on adsorption data that shown here, NZVI particles synthesized by the second method (sample2) are capable to act as an excellent reducing agent when reacted with many compounds. In regards to particle size of Fe<sup>0</sup>, it was also calculated and equaled to 0.647 nm.

### 3.4. The Granule’s Activity:

Its defined as the fragmentation (fracture) of contaminant to the surface of zero nanometric iron. These cracks are used to reduce the contamination based on treatment method with iron. In result, the electrons acquired by polluter upon reduction depend on products formed during this process. Also, the effectiveness of the granule in this has been studied in the presence of carbaryl pesticide (molecular structure) C<sub>12</sub>H<sub>11</sub>NO<sub>2</sub> (figure 6).

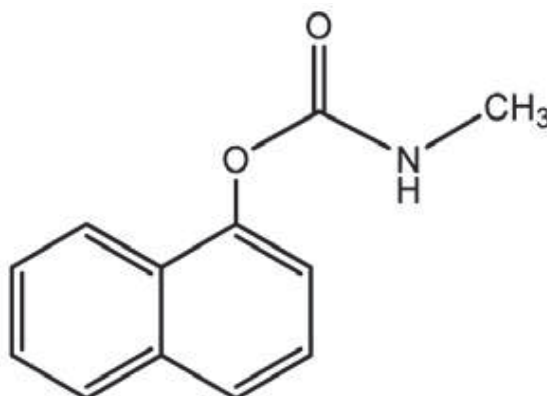


Figure (6) Chemical structure of Carbaryl pesticide

The reaction between NZVI and carbaryl molecules contains gaining an electron and losing the carbamate group which will eventually give 1-Naphthol as seen in figure 7:

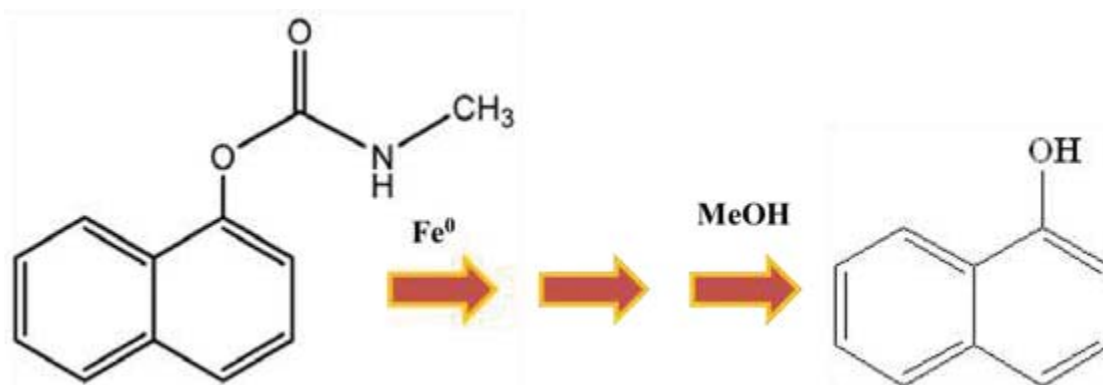


Figure (7)  $\text{Fe}^0$  reaction with Carbaryl pesticide

The granule's activity (E) was then equal to 9.3%.

#### 4. Conclusion:

Via three synthesis methods, NZVI was synthesized and characterized in current study using sodium borohydride as a reducing agent. The first two methods were successfully applied and NZVI was prepared in a good yield. However, the yield of third method showed some rusted parts and quiet low amount not enough for later examination. The existence of NZVI in obtained samples was confirmed by employing XRD, BET, and microscope technologies along with detailed interpretation to figure out the properties of  $\text{Fe}^0$  compounds. The granule's activity was equaled to 9.3% to assess the suitability of currently prepared NZVI powder. On the same hand, the particles size equaled to 6.4 and 0.64 nm for samples 1&2 consequently. The synthesized powder is ready to be used in multiple applications regard environmental remediation from organic and inorganic compounds which will be discussed in our next research.

#### Acknowledgement:

I would like to acknowledge the staff of our college for helping me out to complete this scientific work. Also, I would like to acknowledge Professor Mohsin Al-Dokheily, and Professor Mahmood Shakir for their advice throughout the work.

#### 5. References:

- 1 Pilchin, A. and L. Eppelbaum, Iron and its unique role in Earth evolution. 2006.
- 2 Remediation, U.S.E.P.A.O.o.S. and T. Innovation, Assessing the Use and Application of Zero-valent Iron Nanoparticle Technology for Remediation at Contaminated Sites. 20 :09U.S. Environmental Protection Agency, Office of Superfund Remediation and Technology Innovation.
- 3 Abbaspour, N., R. Hurrell, and R. Kelishadi, Review on iron and its importance for human health. Journal of research in medical sciences : the official journal of Isfahan University of Medical Sciences, 2014. 19(2): p. 164-174.
- 4 Pasinszki, T.K., M. , Synthesis and Application of Zero-Valent Iron Nanoparticles in Water Treatment, Environmental Remediation, Catalysis, and Their Biological Effects. ,. Nanomaterials, 2020. **10**,(9)17.(,
- 5 Introduction to Nanoparticles, in Microwaves in Nanoparticle Synthesis. p. 1-24.

- .6 Keane, E., Fate, Transport and Toxicity of Nanoscale Zero-Valent Iron (nZVI) Used During Superfund Remediation. 2009.
- .7 Jang MH, L.M., Hwang YS. , Potential environmental implications of nanoscale zero-valent iron particles for environmental remediation. . ;29:e2014022. DOI: 10.5620/eht.e2014022.  
.Environmental Health and Toxicology, 2014.
- .8 Fan, L., et al., Promoting the Fe(VI) active species generation by structural and electronic modulation of efficient iron oxide based water oxidation catalyst without Ni or Co. Nano Energy, 2020. **72**: p. 104656.
- .9 Dong, H., et al., *Integration of nanoscale zero-valent iron and functional anaerobic bacteria for groundwater remediation: A review*. Environment International, 2019. **124**: p. 265-277.
- .10 Gheju, M., *Progress in Understanding the Mechanism of CrVI Removal in Fe<sup>0</sup>-Based Filtration Systems*. Water, 2018. **10**: p. 651.